



## OPEN

SUBJECT AREAS:  
PREDICTIVE MARKERS  
GENETIC MARKERSReceived  
20 August 2013Accepted  
24 December 2013Published  
27 January 2014Correspondence and  
requests for materials  
should be addressed to  
N.R.P. (Nicole.  
Phillips@unthsc.edu)

# Simultaneous quantification of mitochondrial DNA copy number and deletion ratio: A multiplex real-time PCR assay

Nicole R. Phillips<sup>1</sup>, Marc L. Sprouse<sup>1</sup> & Rhonda K. Roby<sup>1,2</sup><sup>1</sup>University of North Texas Health Science Center, Department of Molecular and Medical Genetics 3500 Camp Bowie Blvd, Fort Worth, TX 76107, <sup>2</sup>University of North Texas Health Science Center, Institute of Applied Genetics 3500 Camp Bowie Blvd, Fort Worth, TX 76107.

**Mitochondrial dysfunction is implicated in a vast array of diseases and conditions, such as Alzheimer's disease, cancer, and aging. Alterations in mitochondrial DNA (mtDNA) may provide insight into the processes that either initiate or propagate this dysfunction. Here, we describe a unique multiplex assay which simultaneously provides assessments of mtDNA copy number and the proportion of genomes with common large deletions by targeting two mitochondrial sites and one nuclear locus. This probe-based, single-tube multiplex provides high specificity while eliminating well-to-well variability that results from assaying nuclear and mitochondrial targets individually.**

Studies of mitochondrial function are prominent in age-related disease research. Mitochondria are involved in a host of homeostatic and signaling processes which extend well beyond ATP production. The mitochondrial genome (mtGenome) is multi-copy per cell, the number of which varies greatly by cell type. Mitochondrial DNA (mtDNA) is highly susceptible to oxidative damage due to its close proximity to the high concentration of reactive oxygen species (ROS) produced in the mitochondrial matrix and the lack of DNA-protective histones. Additionally, mitochondrial DNA repair mechanisms are less robust than nuclear DNA repair systems, causing damage-induced mutations to remain and potentially propagate. Oxidative damage to DNA results in strand breaks, abasic sites, base changes, and deletions. These processes have been extensively studied and reviewed in the literature, specifically in reference to diseases such as cancer<sup>1–7</sup>. Since there are multiple mtGenomes per cell, it is possible to have a heterogeneous population of mtDNA in cells, tissues and/or organisms, a condition known as heteroplasmy. While heteroplasmy can be inherited at the germline level, it often arises as the result of somatic mutations. Damaged mtDNA molecules can result in malfunctioning proteins and altered mtDNA replication and/or transcription efficiency.

Most mitochondria contain between one and ten copies of mtDNA<sup>8,9</sup>, although the number of which is highly dynamic and regulated in a cell-specific manner by mechanisms that are not completely understood<sup>10,11</sup>. The ratio of mtDNA to nDNA is often used as an estimate for the number of mtGenomes per cell, or mtDNA copy number. This is a high-level indicator of mitochondrial biogenesis as the mtGenome encodes most of the enzymatic subunits of the oxidative phosphorylation system. In addition to mitochondrial DNA depletion syndromes, mtDNA copy number has been investigated in brain tissue and peripheral blood of individuals with impaired cognitive function or late onset Alzheimer's disease<sup>12–14</sup> as well as in various cancer tissues<sup>15–19</sup>.

Large deletions found in the major arc of the mtGenome are causal in many mitochondrial diseases, such as Kearns-Sayre syndrome (KSS), but have also been associated with normal aging processes and age-related diseases in various tissues<sup>20–24</sup>. Most of these deletions have breakpoints associated with repeat motifs, either direct or indirect. A “common” deletion of 4,977 bp that was originally identified in KSS<sup>25</sup> has now been found in varying levels of tissues as they age, specifically in highly energetic, post-mitotic tissues such as brain<sup>26</sup>, skeletal muscle and cardiac muscle. At the time of submission, 131 deletions were reported at [www.MitoMap.org](http://www.MitoMap.org), with 124 deletions contained within the major arc of the mtGenome. Since heteroplasmic populations of mtGenomes can arise when somatic deletions are introduced and clonally expand, the prevalence of deletions within the mtDNA population can vary at the organelle, tissue and/or cellular level. As a result, mitochondrial function may



be unaffected by the existence of such truncated genomes and compensated by the remaining normal mtDNAs, or adversely affected if the number of truncated genomes is too great, causing a deficiency of protein products required for proper oxidative phosphorylation<sup>10,27</sup>.

Here, we discuss a multiplex real-time quantitative PCR (qPCR) assay which simultaneously assesses deletion ratio (mtDNA<sub>DR</sub>) as well as mtDNA copy number (mtDNA<sub>CN</sub>) by targeting three regions: 1) a single-copy nuclear locus, 2) a mitochondrial DNA site in the minor arc where large deletions are rare (mtMinArc), and 3) a mitochondrial DNA site in the major arc where large deletions are common (mtMajArc) (Figure 1). The mtDNA<sub>CN</sub> per cell is represented by the ratio of the mtMinArc target to the nuclear target. The proportion of mtGenomes with major arc deletions, or mtDNA<sub>DR</sub>, is represented by (mtMinArc-mtMajArc)/mtMinArc. Multiplexing the three targets not only offers higher throughput analyses at a reduced cost, but also minimizes extraneous variability due to multiple pipetting and well-to-well variation that occur when comparing multiple singleplex reactions.

## Results

**Design of the mtDNA<sub>CN</sub> and mtDNA<sub>DR</sub> multiplex.** The qPCR targets were strategically selected for this assay. The mtMinArc target is in the D-loop and was chosen because of the rarity, if not absence, of deletions in this region. Although this region is highly polymorphic, the target lies between HV1 and HV2, which is relatively less variable. At the time of submission, no mtDNA deletions have been reported that affect the mtMinArc target, and the primer and probe binding sequences were confirmed to be free of common polymorphic sites<sup>28</sup>. The mtMajArc target is in ND4 and was chosen to lay within the greatest number of reported large deletions in the major arc. Of the 124 major arc deletions, approximately 84% span the mtMajArc target, including the 4977 bp “common deletion”. The nuclear target is within the  $\beta$ 2M gene and was selected because it is single-copy and has low variability, as described by Malik et al., 2011<sup>29</sup>. The primer and probe design for these targets was carefully considered since (1) specific mtDNA amplification in the presence of nDNA is

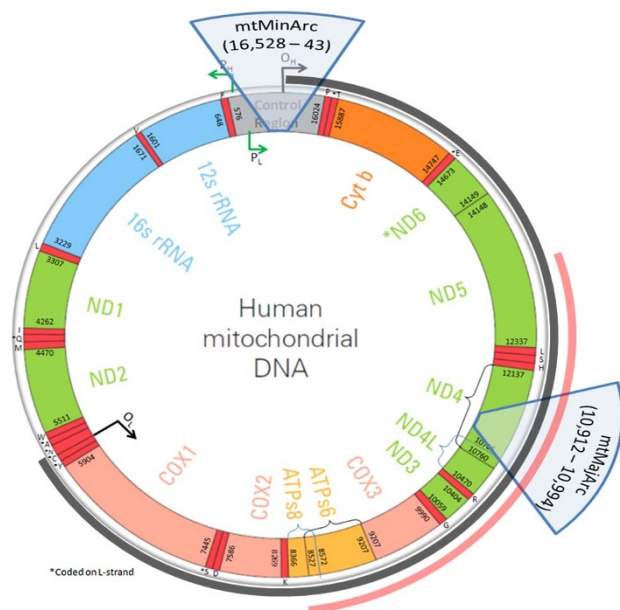


**Figure 1 | Location of mitochondrial targets.** The mtMajArc target is located within the major arc of the mtGenome (denoted by the dark arc between the origins of replication,  $O_H$  and  $O_L$ ). It is spanned by 84% of the reported deletions, including the “common” deletion (denoted by the red arc between positions 8469–13447). The mtMinArc target is located in the D-loop of the mtGenome where no deletions have been reported.

very difficult to achieve, (2) the mtGenome is highly polymorphic, and (3) the amplification strategy is a triplex, requiring selected oligonucleotides to have compatible melting temperatures while minimizing primer-primer and primer-probe interactions. Using a combination of bioinformatic tools, we were able to successfully design the primers and probes for this multiplex (Table 1). The absence of pseudogene amplification was verified in both samples, as evidenced by the expected alignment of the sequence data with the whole human genome using BLAST and the lack of mixed bases in the resulting sequence data. A negative (no template) control performed as expected.

In our laboratory, we have demonstrated that synthetic standards in multiplex reactions are amplified with a high degree of variability (data not shown), and circular plasmid standards may result in absolute quantification errors<sup>30</sup>. For these reasons, and the fact that we use this assay primarily for the assessment of peripheral blood extracts, we elected to conduct absolute quantification by creating standards from a concentrated peripheral blood extract in order to ensure that our standard curves are representative of the samples tested. The Standard 1 concentrations for the nuclear and mtDNA targets were determined by independent qPCR assays, the results of which were verified to correspond well with an alternative quantification method, QX100™ Droplet Digital™ PCR (ddPCR) (Bio-Rad Laboratories, Hercules, CA). The nDNA qPCR singleplex assay estimate was 1.36× higher than the ddPCR result, and the mtDNA qPCR singleplex assay estimate was 1.55× higher than the ddPCR result. Importantly, the mtDNA copy number ratio was essentially unaltered when comparing the two methods (1.14× higher estimate by qPCR). Since these two measures were very similar, the standard curve was calibrated on the singleplex qPCR assay results. The dynamic range of the standard curve was intentionally limited in order to most accurately quantify our samples of interest, which have concentrations within a limited range. The 95% confidence intervals for the Ct values of each standard in the linear range of the assay were constructed based on sixteen replicate tests (Figure 2). The greatest observed margin of error was 0.32, for Standard 8 of  $\beta$ 2M, which is expected of the lower concentrations in the linear range. High amplification efficiency and correlation coefficients were obtained for all of the multiplex targets.

**Repeatability and reproducibility.** Acceptable repeatability and reproducibility of each of the three targets are indicated by the low intra- and inter-assay variability in quantification cycle (Cq) observed (Table 2 and Figure 3). For the repeatability test, two replicates (each from a different sample) qualified as outliers and were omitted. The standard deviations of replicates within one run are such that each sample concentration is distinguishable with greater than 99.7% confidence (mean  $\pm$  3SD). Reproducibility of each qPCR target and mtDNA copy number per cell was demonstrated as well. The relative mtDNA copy numbers, calculated as the ratio of mtMinArc to  $\beta$ 2M, were analyzed, and the 95% confidence intervals constructed for each nine replicates of eight samples indicate that the variability between runs is small. No significant difference in mean mtDNA copy number was observed between values obtained from three independent runs (one-way ANOVA,  $p$ -value = 0.979); furthermore, no significant difference between the triplicate tests within each run was observed (one-way ANOVA,  $p$ -values were 0.996, 0.811, 0.940 for runs 1, 2, and 3, respectively).

**Mitochondrial DNA copy number accuracy.** A difference in quantification results was indicated in a 10-sample training set when using the multiplex assay as compared to individual ddPCR assays. Both mitochondrial and nuclear DNA estimates were higher using the multiplex reaction by an average of 2.46× (SD = 0.5176) and 1.79× (SD = 0.3192), respectively. This is likely due to amplification bias in the multiplex reaction and the intentionally limited mtDNA primer concentrations. Importantly, however, mtDNA<sub>CN</sub> was not affected and was shown to be statistically equivalent when

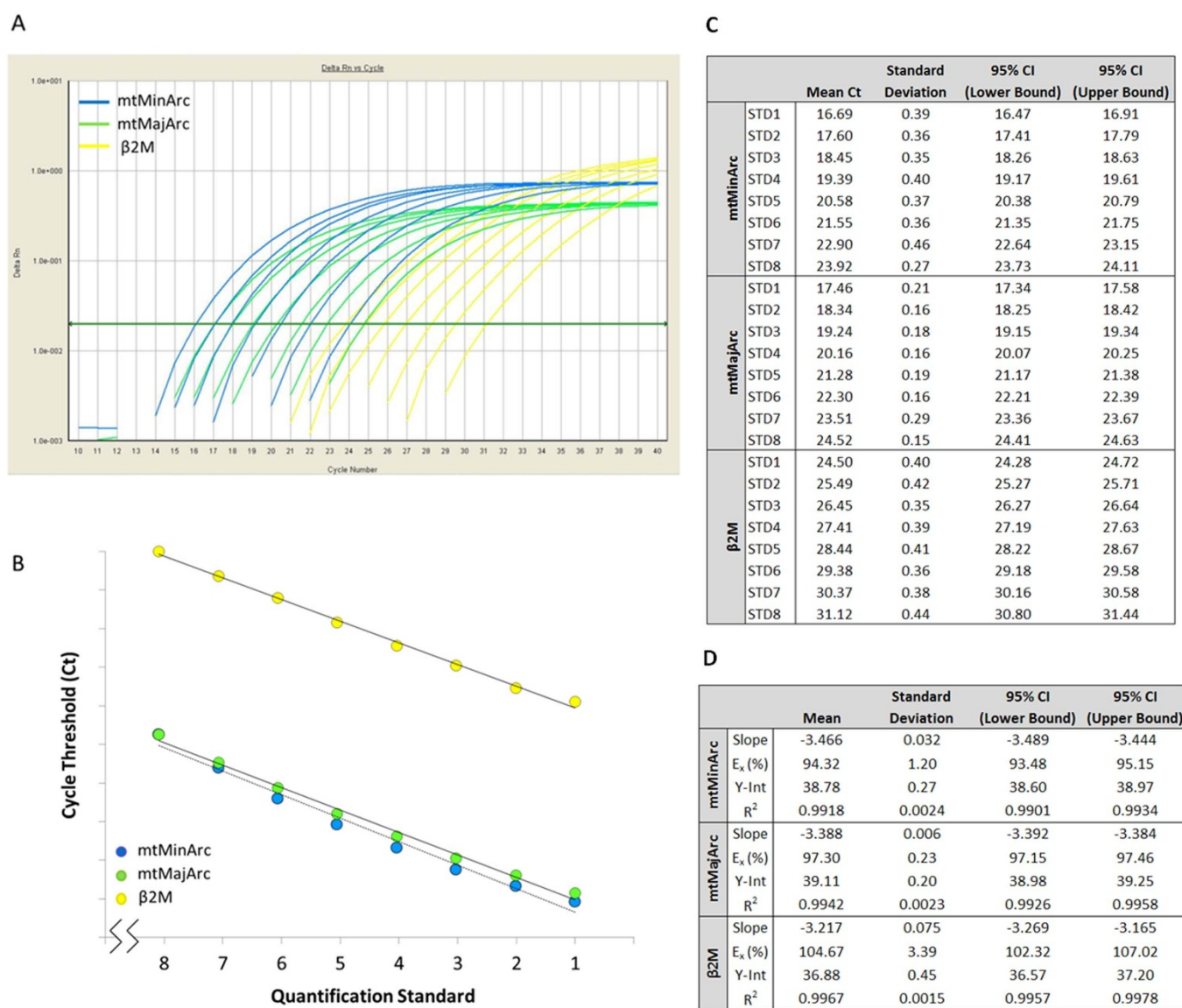


**Table 1** | Specification of primer and probe nucleotide sequences.  $\beta$ 2M positions refer to NT\_010194.17 as previously published by Malik et al., 2011; mtDNA positions refer to NC\_012920

Primer Name	Binding Site Positions	Sequence (5'-3')
FmtMinArc	mt 16,528 – 16,548	CTAAATAGCCCACACGTTCCC
RmtMinArc	mt 23 – 42	AGAGCTCCCGTGAGTGGTTA
FmtMajArc	mt 10,912 – 10,931	CTGTTCCCAACCTTTTCT
RmtMajArc	mt 10,975 – 10,994	CCATGATTGTGAGGGGTAGG
F $\beta$ 2M	Chr15 15,798,932 – 15,798,958	GCTGGGTAGCTCTAAACAATGTATTCA
R $\beta$ 2M	Chr15 15,798,999 – 15,799,026	CCATGTACTAACAAATGTCTAAAATGGT

Probe Name	Binding Site Positions	Sequence (5'-3')
PmtMinArc	mt 16,560 – 10	6FAM-CATCACGATGGATCACAGGT(NFQ)
PmtMajArc	mt 10,934 – 10,951	NED-GACCCCCTAACACCCCC(NFQ)
P $\beta$ 2M	Chr15 15,798,969 – 15,798,984	VIC-CAGCAGCCTATTCTGC(NFQ)



**Figure 2** | Standard curve reproducibility. *Panel A* - A representative real-time amplification plot of the standard DNA dilution series. The green horizontal line indicates the manual Cq threshold set at 0.04. *Panel B* - A representative standard curve regression. Note that the Y-intercept (provided in the table) is a function of the concentration of the standards; however, since the data are plotted by quantification standard number, the Y-intercepts are misrepresented (denoted by the broken x-axis). *Panel C* - Descriptive statistics for sixteen replicate standard curves analyzed on eight separate runs. *Panel D* - Descriptive statistics for the slope, amplification efficiency (E<sub>x</sub>), Y-intercept (Y-int.), and correlation coefficient (R<sup>2</sup>) for eight runs with the standard curve analyzed in duplicate. All three targets are optimized, as indicated by the high R<sup>2</sup> value ( $\geq 0.99$ ) and high amplification efficiency ( $> 90\%$ ). CI, confidence interval.





**Table 2 |** Repeatability of the multiplex assay. Seven samples (A–G) were amplified in six replicates on a single run to assess the intra-assay variability. Samples A through G are ranked by concentration, with A being the most concentrated and G being the least. The mean, standard deviation (SD), minimum (Min), and maximum (Max) of the C<sub>q</sub> values are provided for each target

		A	B	C	D	E	F	G
<b>mtMinArc</b>	Mean	20.90	21.66	22.62	23.70	24.88	26.31	27.83
	SD	0.15	0.10	0.13	0.17	0.16	0.10	0.13
	Min	20.67	21.52	22.48	23.46	24.71	26.18	27.71
	Max	21.12	21.77	22.81	23.97	25.08	26.47	28.04
<b>mtMajArc</b>	Mean	22.81	23.57	24.54	25.58	26.69	28.01	29.39
	SD	0.21	0.19	0.18	0.20	0.22	0.21	0.18
	Min	22.60	23.34	24.34	25.39	26.47	27.78	29.21
	Max	23.14	23.84	24.78	25.83	26.99	28.27	29.63
<b>β2M</b>	Mean	28.80	29.65	30.66	31.68	32.68	33.70	35.02
	SD	0.16	0.10	0.06	0.05	0.07	0.14	0.14
	Min	28.64	29.56	30.60	31.61	32.59	33.45	34.83
	Max	29.03	29.81	30.75	31.73	32.77	33.83	35.19

assessed using the multiplex and independent quantitative assays (two sample paired t-test for means, two-tailed p-value 0.1307; data not shown).

**Mitochondrial DNA deletion ratio accuracy and resolution.** The deletion ration for the mtDNA sample known to harbor a large deletion (mtDNA<sub>Del</sub>) was quantified as 61.5% using the multiplex assay. A series of DNA mixtures were created to test the resolution of deletion detection. Data from the mixture series experiments met the assumption of normality, and the mixture tests indicated that the

multiplex assay can detect significant differences in mtDNA<sub>DR</sub> between samples that differ by 12.0% ( $p < 0.0005$ ), 10.0% ( $p = 0.013$ ), 8.7% ( $p = 0.085$ ), and 5.9% ( $p = 0.017$ ). At 4.4%, there was no significant difference between the two samples ( $p = 0.990$ ) (Figure 4). These results indicate that the assay can resolve samples which differ in deletion ratio by at least 5.9%.

## Discussion

The main objective of the assay design was to assess mtDNA alterations that may be a result of age-related increase in oxidative stress.

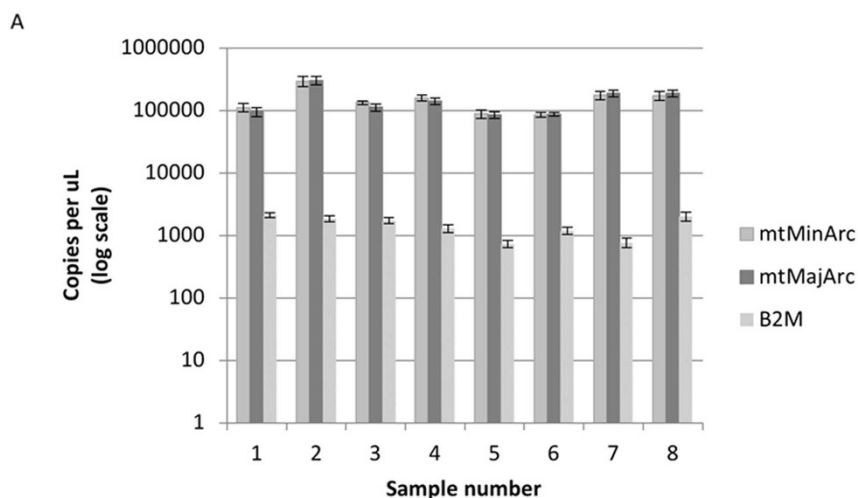


**Figure 3 |** Reproducibility of the multiplex assay. Absolute quantification was performed on eight samples (1–8) amplified in triplicate on three separate runs (nine replicates per sample) in order to assess the inter-assay variability. *Panel A*– The mean and standard deviation for each target are provided for each sample. *Panel B*– Descriptive statistics for mtDNA copy number of the nine replicates, calculated by the ratio of the mtMinArc target quantification result to the β2M quantification result. CI, confidence interval.

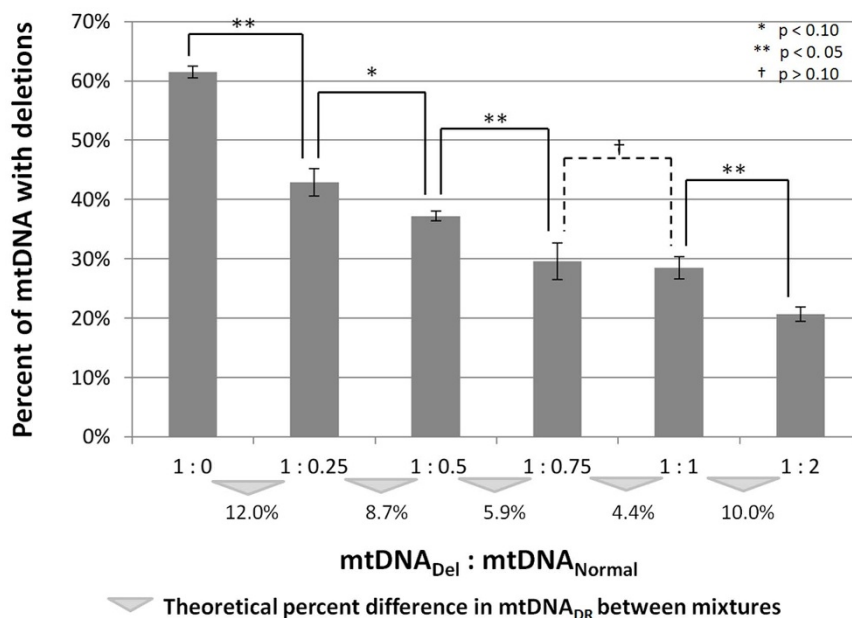


**Figure 4 | Assessment of major arc deletion detection resolution using a mixture series.** Two samples, one which harbors a major arc deletion at 61.5% heteroplasmy (mtDNA<sub>Del</sub>) based on the multiplex quantification of the 1 : 0 neat sample, and one which does not harbor a known deletion (mtDNA<sub>Normal</sub>), were mixed in varying proportions and analyzed in triplicate. The theoretical difference in mtDNA deletion ratio (mtDNA<sub>DR</sub>) between each sample type is denoted with a triangle. Significant differences ( $\alpha = 0.10$ ) between the samples of varying deletion ratios are indicated with the brackets and asterisks; no significant difference was observed between the 1 : 0.75 mixture and the 1 : 1 mixture, the two mixtures which theoretically differ the least (mtDNA<sub>DR</sub> difference of 4.4%). Therefore, this assay can detect differences in deletion ratio  $\geq 5.9\%$ .

While there are many published methods for detecting mtDNA variation, generally, the previously described methods do not meet the goals addressed in this assay in at least one of the following areas: 1) detection of multiple deletions rather than specific break points, 2) elimination of well-to-well variability through probe-based multiplexing, and/or 3) simultaneous assessment of both mtDNA copy number and mtDNA deletion ratio. Primary mitochondrial diseases have typically been diagnosed by detection of specific mtDNA mutations and deletions using Southern blot techniques. This procedure requires a large amount of DNA and is limited in sensitivity. More recently, there have been many published qPCR assays that test for specific pathological mtDNA point mutations and deletions that are associated with various diseases and/or aging<sup>27,31–34</sup>. The multiplex assay described here targets a region in the mtGenome that is inclusive to 84% of the reported deletions while also providing assessment of mtDNA copy number per cell. These measures of mtGenome integrity have great utility in many areas of biomedical research. The data presented here indicate that the assay is both accurate and sensitive in these two assessments with the valuable added benefits of multiplexing (*i.e.*, reduced cost, increased throughput, and importantly, decreased variability due to multiple pipetting and well-to-well differences). We present this assay as an efficient and effective tool for biomedical researchers interested in assessing mtDNA changes associated with various aging and disease processes.

## Methods

**Samples.** Informed consent was obtained for all of the subjects included in this study; methods for subject recruitment and testing were approved by the Office of the Protection of Human Subjects-Institutional Review Board (Project #2010-120 and Project #2012-094; UNT Health Science Center, Fort Worth, TX). All experiments were conducted in the investigator's laboratory.

**Design of the mtDNA<sub>CN</sub> and mtDNA<sub>DR</sub> multiplex.** The mitochondrial targets are novel and were carefully selected with regard to the location of reported deletions within the mtGenome. The mtMinArc target spans the heavy strand origin of replication and is not affected by any of the reported large deletions. The mtMajArc target lies within the "common" deletion as well as within 84% of the reported large deletions in the major arc (Figure 1). Primers and probes were designed using

Primer3 (Whitehead Institute for Biomedical Research, Cambridge, MA), Primer-BLAST/BLAST (National Center for Biotechnology Information, Bethesda, MD), and Oligo Analyzer 3.1 (Integrated DNA Technologies Inc, Coralville, IA) (Table 1). Using these bioinformatic tools, the primers and probes were tested for compatibility as well as non-specific amplification. Additionally, the mtMinArc primers were screened for common population polymorphisms using the "mtDNA Population Database" since they bind in the hypervariable control region<sup>28</sup>. Two samples, a blood DNA extract and HL60 cell line control DNA, were amplified using the mtDNA primers under analogous PCR conditions to the qPCR protocol. The products were sequenced using BigDye<sup>®</sup> Terminator v1.1 Cycle Sequencing Kit (Applied Biosystems)<sup>35</sup> in order to confirm the specific amplification of the mitochondrial targets. The sequence data were (1) aligned to the human genome using BLAST to confirm that the intended target was amplified, and (2) analyzed for the presence of mixed bases, indicating contaminating amplification products. The  $\beta 2M$  primers and probe sequences have been previously described<sup>29</sup>.

Real-time PCR of the three targets was performed using a probe-based multiplex qPCR assay on the 7500 Real-Time PCR System (Applied Biosystems, Foster City, CA) using the following thermal profile: 95 °C for 10 min; 40 cycles of 95 °C for 15 s, 55 °C for 15 s; and 60 °C for 1 min. The reaction components are as follows (given in final concentration): 22.5  $\mu$ L TaqMan<sup>®</sup> Universal PCR Master Mix, No AmpErase<sup>®</sup> UNG (Applied Biosystems), each mitochondrial primer at 50 nM (FmtMinArc, RmtMinArc, FmtMajArc, RmtMajArc), each nuclear DNA primer at 1250 nM (F $\beta 2M$ , R $\beta 2M$ ), and each dual hybridization probe at 250 nM (PmtMinArc, PmtMajArc, P $\beta 2M$ ) (TaqMan<sup>®</sup> MGB Probe, Applied Biosystems). The final reaction volume is 25  $\mu$ L. Absolute quantification was obtained using a standard curve generated from a reference DNA sample from a healthy, 30-year-old male. Whole blood was extracted using the QIAmp<sup>®</sup> DNA Blood Mini Kit (Qiagen, Inc., Hilden, Germany) and the respective DNA concentrations were then measured independently using the following singleplex qPCR assays: mtDNA was quantified using a mtDNA qPCR assay<sup>36</sup> and nuclear DNA was quantified using Quantifiler<sup>®</sup> Duo DNA Quantification Kit (Applied Biosystems). The sample was concentrated and re-quantified (using the same aforementioned singleplex qPCR assays) to generate the first standard, Std1, with a target concentration of approximately 7000 cells/ $\mu$ L and 2.7 million mtDNA copies/ $\mu$ L (exact quantification values used for absolute quantification). Four replicates of Std 1 were assayed using the ddPCR System, according to the manufacturer's protocol, to quantify each target concentration. The same nDNA and mtDNA major arc primers and probes designed for the multiplex were used for the ddPCR tests (Table 1). These results were compared to singleplex qPCR results and used to calibrate the standard curve quantification values used for the multiplex assay. A two-fold dilution series of Std1 was used to create the subsequent standards (Std2-Std8). Standard curves were analyzed at a Cq of 0.04, using the automatic baselining algorithm. Sixteen replicate tests of the standard curve (two standards on each of eight runs) were analyzed for reproducibility, amplification efficiency and correlation. 95% confidence intervals were constructed for the Ct values of each standard within the linear range. Additionally, 95% confidence



intervals were constructed for the amplification efficiency ( $E_x$ ), Y-intercept and correlation ( $R^2$ ) of each pair of standards (*i.e.*, for each of the eight runs). High amplification efficiency was obtained for all of the multiplex targets, as indicated by the slope (Figure 2). The amplification efficiency, Y-intercept and  $R^2$  values were analyzed for all standard curves prior to absolute quantification of unknown samples.

**Repeatability and reproducibility.** In order to assess the intra-assay reproducibility, a two-fold dilution series was performed to create seven samples of varying concentration (A–G); each was amplified in six replicates. The mean, standard deviation, minimum and maximum of the Cq values were obtained for all targets of each sample (Table 2). Inter-assay variability was assessed by performing absolute quantification of eight samples (1–8) in triplicate on three separate runs. Replicate outliers were omitted where quantification values exceeded 1.5 times the interquartile range limits. The mean and standard deviation were calculated for all targets of each sample (Figure 3, Panel A). MtDNA copy number was derived from the ratio of the mtMinArc target quantification result to the  $\beta$ 2M target quantification result for each replicate of the eight samples, and 95% confidence intervals were constructed to assess reproducibility of the mtDNA copy number per cell ratio (Figure 3, Panel B). One-way ANOVA tests were performed to determine if significant differences in mtDNA copy number were observed between replicates within and between runs.

**Mitochondrial DNA copy number accuracy.** Ten peripheral blood buffy coat samples were extracted, quantified by NanoDrop® Spectrophotometer (Thermo Fisher Scientific Inc., Waltham, MA), and normalized to 10 ng/ $\mu$ L. Mitochondrial DNA copy number was independently quantified for each of the ten samples, assayed in triplicate, using the ddPCR System according to the manufacturer's protocol. The same nDNA and mtDNA major arc primers and probes were used as designed for the multiplex (Table 1). The number of mtGenomes was extrapolated from the concentration of mtDNA, given that 1 pg of mtDNA contains approximately 58,800 mtGenomes, as manually calculated using the nucleotide sequence of NC\_012920<sup>37</sup>. The number of cells was extrapolated from the concentration of nDNA, assuming there is 6.5 pg nDNA in one diploid cell<sup>38,39</sup>. Dividing the resulting number of mtGenomes by the number of cells represents the mitochondrial DNA copy number obtained by individual reactions. The same ten DNAs were used in the single-tube multiplex assay (described above in *Multiplexed mtDNA<sub>CN</sub> and Deletion Ratio Assay*). The mtDNA, nDNA, and mtDNA copy number results from the two methods were compared using paired t-tests.

**Mitochondrial DNA deletion ratio accuracy and resolution.** DNA extracted from a cybrid cell line known to harbor a large deletion in the major arc<sup>39</sup> was assayed with this multiplex. The deletion ratio was estimated by Southern blot and real-time qPCR analysis to contain approximately 70% mtDNA genomes with a 7.5 kb deletion between positions 7982–15504 (mtDNA<sub>Del</sub>). While not the “common” 4,977 bp deletion, this larger deletion has previously been detected in patients with KSS<sup>40–42</sup>. In order to assess the resolution of detecting differences in mtDNA<sub>DR</sub>, a mixture series using the mtDNA<sub>Del</sub> sample was created. This sample was mixed with the reference standard described previously, which is assumed to harbor no mtDNA deletions (mtDNA<sub>Norm</sub>). Six ratios, ranging from 1:0 to 1:2 (mtDNA<sub>Del</sub>:mtDNA<sub>Norm</sub>), were tested in triplicate to determine the resolution of mtDNA deletion detection. The theoretical deletion ratio (mtDNA<sub>DR</sub>) was calculated for each sample based on the multiplex quantification result of the neat mtDNA<sub>Del</sub> sample (1:0), and the difference in mtDNA<sub>DR</sub> between each mixture was determined as marked with the triangle in Figure 4. The differences in mtDNA<sub>DR</sub> range from 4.4–12.0%. Normality was tested using Kolmogorov-Smirnov method, and a one-way ANOVA was performed using Tukey HSD for post hoc analyses.

**Data analysis.** Statistical analyses were performed using IBM® SPSS™ Statistics 19 (IBM Corporation, Armonk, NY) and Microsoft Excel® Data Analysis Tools (Microsoft Corporation, Redmond, WA).

- Ames, B. N., Shigenaga, M. K. & Hagen, T. M. Oxidants, antioxidants, and the degenerative diseases of aging. *Proc. Natl. Acad. Sci. U.S.A.* **90**, 7915–7922 (1993).
- Dreher, D. & Junod, A. Role of oxygen free radicals in cancer development. *Eur. J. Cancer* **32**, 30–38 (1996).
- Henle, E. S. & Linn, S. Formation, prevention, and repair of DNA damage by iron/hydrogen peroxide. *J. Biol. Chem.* **272**, 19095–19098 (1997).
- Loft, S. & Poulsen, H. Cancer risk and oxidative DNA damage in man. *J. Mol. Med.* **74**, 297–312 (1996).
- Richter, C., Park, J. W. & Ames, B. N. Normal oxidative damage to mitochondrial and nuclear DNA is extensive. *Proc. Natl. Acad. Sci. U.S.A.* **85**, 6465–6467 (1988).
- Wiseman, H., Kaur, H. & Halliwell, B. DNA damage and cancer: measurement and mechanism. *Cancer Lett.* **93**, 113–120 (1995).
- Yakes, F. M. & Van Houten, B. Mitochondrial DNA damage is more extensive and persists longer than nuclear DNA damage in human cells following oxidative stress. *Proc. Natl. Acad. Sci. U.S.A.* **94**, 514–519 (1997).
- Robin, E. D. & Wong, R. Mitochondrial DNA molecules and virtual number of mitochondria per cell in mammalian cells. *J. Cell. Physiol.* **136**, 507–513 (1988).
- Satoh, M. & Kuroiwa, T. Organization of multiple nucleoids and DNA molecules in mitochondria of a human cell. *Exp. Cell Res.* **196**, 137–140 (1991).
- Clay Montier, L. L., Deng, J. J. & Bai, Y. Number matters: control of mammalian mitochondrial DNA copy number. *J. Genet. Genomics* **36**, 125–131 (2009).

- Gianotti, T. F. *et al.* Mitochondrial DNA copy number is modulated by genetic variation in the signal transducer and activator of transcription 3 (STAT3). *Metab. Clin. Exp.* **60**, 1142–1149 (2011).
- Coskun, P. E. *et al.* Systemic Mitochondrial Dysfunction and the Etiology of Alzheimer's Disease and Down Syndrome Dementia. *J. Alzheimer's Dis.* **20**, 293–310 (2010).
- Hirai, K. *et al.* Mitochondrial abnormalities in Alzheimer's disease. *J. Neurosci.* **21**, 3017–3023 (2001).
- Swerdlow, R. H. Is aging part of Alzheimer's disease, or is Alzheimer's disease part of aging? *Neurobiol. Aging* **28**, 1465–1480 (2007).
- Chan, S. W. *et al.* Mitochondrial DNA damage is sensitive to exogenous H<sub>2</sub>O<sub>2</sub> but independent of cellular ROS production in prostate cancer cells. *Mutat. Res., Fundam. Mol. Mech. Mutagen.* **716**, 40–50 (2011).
- Higuchi, M. Regulation of mitochondrial DNA content and cancer. *Mitochondrion* **7**, 53–57 (2007).
- Mizumachi, T. *et al.* Increased distributional variance of mitochondrial DNA content associated with prostate cancer cells as compared with normal prostate cells. *Prostate* **68**, 408–417 (2008).
- Xing, J. *et al.* Mitochondrial DNA content: its genetic heritability and association with renal cell carcinoma. *J. Natl. Cancer Inst.* **100**, 1104–1112 (2008).
- Yu, M. *et al.* Reduced mitochondrial DNA copy number is correlated with tumor progression and prognosis in Chinese breast cancer patients. *IUBMB Life* **59**, 450–457 (2007).
- Aliev, G. *et al.* Atherosclerotic lesions and mitochondria DNA deletions in brain microvessels: Implication in the pathogenesis of Alzheimer's disease. *Vasc. Health Risk Manage.* **4**, 721–730 (2008).
- Corral-Debrinski, M. *et al.* Marked changes in mitochondrial DNA deletion levels in Alzheimer brains. *Genomics* **23**, 471–476 (1994).
- Lee, H. C., Chang, C. M. & Chi, C. W. Somatic Mutations of Mitochondrial DNA in Aging and Cancer Progression. *Ageing Res. Rev.* **9**, S47–S58 (2010).
- Miller, B. & Bennett, J. P. The locus ceruleus contains mitochondrial DNA deletions in Alzheimer's Disease. *Mitochondrion* **10**, 239–240 (2010).
- Reguly, B., Jakupciak, J. P. & Parr, R. L. 3.4 kb mitochondrial genome deletion serves as a surrogate predictive biomarker for prostate cancer in histopathologically benign biopsy cores. *Canadian Urol. Assoc. J.* **4**, E118–E122 (2010).
- Moraes, C. T. *et al.* Mitochondrial DNA deletions in progressive external ophthalmoplegia and Kearns-Sayre syndrome. *N. Engl. J. Med.* **320**, 1293–1299 (1989).
- Phillips, N. R., Simpkins, J. W. & Roby, R. K. Mitochondrial DNA deletions in Alzheimer's brains: A review. *Alzheimer's Dementia*, In press, (2013).
- Bai, R. & Wong, L. C. Simultaneous detection and quantification of mitochondrial DNA deletion (s), depletion, and over-replication in patients with mitochondrial disease. *J. Mol. Diagn.* **7**, 613–622 (2005).
- Monson, K. L., Miller, K. W. P., Wilson, M. R., DiZinno, J. A. & Budowle, B. The mtDNA population database: an integrated software and database resource for forensic comparison. *Research and Technology* **4**, (2002).
- Malik, A. N., Shahni, R., Rodriguez-de-Ledesma, A., Laftah, A. & Cunningham, P. Mitochondrial DNA as a non-invasive biomarker: Accurate quantification using real time quantitative PCR without co-amplification of pseudogenes and dilution bias. *Biochem. Biophys. Res. Commun.* **412**, 1–7 (2011).
- Hou, Y., Zhang, H., Miranda, L. & Lin, S. Serious overestimation in quantitative PCR by circular (supercoiled) plasmid standard: microalgal pcna as the model gene. *PLoS One* **5**, e9545 (2010).
- Harbottle, A. & Birch-Machin, M. Real-time PCR analysis of a 3895 bp mitochondrial DNA deletion in nonmelanoma skin cancer and its use as a quantitative marker for sunlight exposure in human skin. *Br. J. Cancer* **94**, 1887–1893 (2006).
- Krishnan, K. J., Bender, A., Taylor, R. W. & Turnbull, D. M. A multiplex real-time PCR method to detect and quantify mitochondrial DNA deletions in individual cells. *Anal. Biochem.* **370**, 127–129 (2007).
- Poe, B. G., Navratil, M. & Arriaga, E. A. Absolute quantitation of a heteroplasmic mitochondrial DNA deletion using a multiplex three-primer real-time PCR assay. *Anal. Biochem.* **362**, 193–200 (2007).
- Szuhaik, K. *et al.* Simultaneous A8344G heteroplasmy and mitochondrial DNA copy number quantification in myoclonus epilepsy and ragged-red fibers (MERRF) syndrome by a multiplex molecular beacon based real-time fluorescence PCR. *Nucleic Acids Res.* **29**, e13–e13 (2001).
- Roby, R. K., Phillips, N. R., Thomas, J. L., Sprouse, M. & Curtis, P. Development of an Integrated Workflow from Laboratory Processing to Report Generation for mtDNA Haplotype Analysis. *NCJRS* (2011).
- Kavlick, M. F. *et al.* Quantification of Human Mitochondrial DNA Using Synthesized DNA Standards. *J. Forensic Sci.* **56**, 1457–1463 (2011).
- Stothard, P. The sequence manipulation suite: JavaScript programs for analyzing and formatting protein and DNA sequences. *BioTechniques* **28**, 1102–1104 (2000).
- Dolezel, J., Bartos, J., Voglmayr, H. & Greilhuber, J. Nuclear DNA content and genome size of trout and human. *Cytometry A* **51**, 127–128.
- Moraes, C. T., Kenyon, L. & Hao, H. Mechanisms of human mitochondrial DNA maintenance: the determining role of primary sequence and length over function. *Mol. Biol. Cell* **10**, 3345–3356 (1999).



40. Mita, S. *et al.* Recombination via flanking direct repeats is a major cause of large-scale deletions of human mitochondrial DNA. *Nucleic Acids Res.* **18**, 561–567 (1990).
41. Nakase, H. *et al.* Transcription and translation of deleted mitochondrial genomes in Kearns-Sayre syndrome: implications for pathogenesis. *Am. J. Hum. Genet.* **46**, 418–427 (1990).
42. Zupanc, M. L. *et al.* Deletion of mitochondrial DNA in patients with combined features of Kearns-Sayre and MELAS syndromes. *Ann. Neurol.* **29**, 680–683 (1991).

## Acknowledgments

We would like to acknowledge the contribution of Dr. Carlos Moraes and Dr. Milena Pinto at the University of Miami Miller School of Medicine for their donation of the cybrid DNA. Additionally, we would like to acknowledge Dr. Michael Allen and his laboratory at the University of North Texas Health Science Center for their assistance with the ddPCR experiments. This project was funded in part by the following awards: Alzheimer's

Association NIRG-12-242728; UNTHSC Intramural Seed Grant, 2012–2013; National Institute of Aging, Training in the Neurobiology of Aging T32 AG 020494.

## Author contributions

N.P. and M.S. conducted all experiments. All authors contributed to the design of the assay and discussed the results. N.P. was the primary author of the manuscript; M.S. and R.R. commented on the manuscript at all stages.

## Additional information

**Competing financial interests:** The authors declare no competing financial interests.

**How to cite this article:** Phillips, N.R., Sprouse, M.L. & Roby, R.K. Simultaneous quantification of mitochondrial DNA copy number and deletion ratio: A multiplex real-time PCR assay. *Sci. Rep.* **4**, 3887; DOI:10.1038/srep03887 (2014).



This work is licensed under a Creative Commons Attribution-NonCommercial-NoDerivs 3.0 Unported license. To view a copy of this license, visit <http://creativecommons.org/licenses/by-nc-nd/3.0>